


Dear Author,

Please, note that changes made to the HTML content will be added to the article before publication, but are not reflected in this PDF.

Note also that this file should not be used for submitting corrections.

**AUTHOR QUERY FORM**

	<b>Journal:</b> HE  <b>Article Number:</b> 14817	<b>Please e-mail or fax your responses and any corrections to:</b>  <b>E-mail:</b> <a href="mailto:corrections.essd@elsevier.tnq.co.in">corrections.essd@elsevier.tnq.co.in</a>  <b>Fax:</b> +31 2048 52789
---	--	---

Dear Author,

Please check your proof carefully and mark all corrections at the appropriate place in the proof (e.g., by using on-screen annotation in the PDF file) or compile them in a separate list. Note: if you opt to annotate the file with software other than Adobe Reader then please also highlight the appropriate place in the PDF file. To ensure fast publication of your paper please return your corrections within 48 hours.

For correction or revision of any artwork, please consult <http://www.elsevier.com/artworkinstructions>.

Any queries or remarks that have arisen during the processing of your manuscript are listed below and highlighted by flags in the proof.

<b>Location in article</b>	<b>Query / Remark: Click on the Q link to find the query's location in text Please insert your reply or correction at the corresponding line in the proof</b>
<b>Q1</b>	Please check the affiliations 'a' and 'b', and amend as necessary.
<b>Q2</b>	Please provide the grant number for 'Conicet' and 'CNEA' if any.
<b>Q3</b>	Please update Ref. [4].
<b>Q4</b>	Please provide a definition for the significance of bold in Table 2.
<b>Q5</b>	Please confirm that given names and surnames have been identified correctly.
	<div data-bbox="304 1300 895 1481" style="border: 1px solid black; padding: 5px;"> <p data-bbox="312 1342 715 1434">Please check this box or indicate your approval if you have no corrections to make to the PDF file</p> <div data-bbox="791 1364 879 1442" style="border: 1px solid black; width: 55px; height: 37px; display: inline-block; vertical-align: middle;"></div> </div>

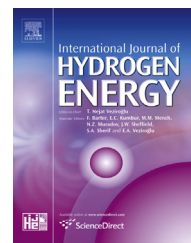
Thank you for your assistance.



ELSEVIER

Available online at [www.sciencedirect.com](http://www.sciencedirect.com)

ScienceDirect

journal homepage: [www.elsevier.com/locate/he](http://www.elsevier.com/locate/he)

## Highlights

- A non dimensional method to estimate reaction time of hydride containers is used.
- Predictions and experimental outcomes are in agreement.
- The prototype hydride container is optimized for 3 min absorption.

UNCORRECTED PROOF

<http://dx.doi.org/10.1016/j.ijhydene.2014.10.027>

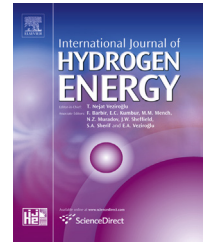
0360-3199/Copyright © 2014, Hydrogen Energy Publications, LLC. Published by Elsevier Ltd. All rights reserved.

Please cite this article in press as: Silin N, Melnichuk M, A case study of a hydride container performance applying non dimensional parameters, International Journal of Hydrogen Energy (2014), <http://dx.doi.org/10.1016/j.ijhydene.2014.10.027>

20  
21  
22  
23  
24  
25  
26  
27  
28  
29  
30  
31  
32  
33  
34  
35  
36  
37  
38  
39

Available online at [www.sciencedirect.com](http://www.sciencedirect.com)

ScienceDirect

journal homepage: [www.elsevier.com/locate/ijhydene](http://www.elsevier.com/locate/ijhydene)

# A case study of a hydride container performance applying non dimensional parameters

N. Silin<sup>a,b,\*</sup>, M. Melnichuk<sup>a,c</sup><sup>a</sup> CONICET, Consejo Nacional de Investigaciones Científicas y Técnicas, Argentina<sup>b</sup> Instituto Balseiro, Centro Atómico Bariloche, Comisión Nacional de Energía Atómica, Universidad Nacional de Cuyo, Av. E. Bustillo 9500, CP 8400 S.C. de Bariloche, Río Negro, Argentina<sup>c</sup> Comisión Nacional de Energía Atómica, Av. E. Bustillo 9500, CP 8400 S.C. de Bariloche, Río Negro, Argentina

## ARTICLE INFO

### Article history:

Received 7 April 2014

Received in revised form

2 October 2014

Accepted 6 October 2014

Available online xxx

### Keywords:

Hydrogen storage

Hydride container

Heat transfer

Design

Non dimensional parameters

## ABSTRACT

Many efforts have been done so far to understand sorption dynamics of hydride containers for hydrogen storage. Particularly, there are many articles in literature where experimental results for different hydride systems and container set-ups were successfully simulated using basically the same group of models. This fact is the base of a previous work where we defined a series of non dimensional parameters which may be used to estimate absorption time of hydride containers.

In this work we compare estimated absorption times with experimental outcomes for a prototype hydride container. We performed non dimensional analysis of our finned container prototype at two scales, i.e.: overall or macroscopic container scale and pore or microscopic scale. We discuss about this simplified model approach that allows estimating, with few parameters, the reaction time of a complex-geometry prototype.

The prototype container was designed according to the results of a numerical optimization that maximized the amount of hydrogen absorbed for a 3 min charging period. Experimental results indicate good agreement between estimated and experimental absorption time, making the non dimensional method a useful tool at preliminary stages of hydride container design.

Copyright © 2014, Hydrogen Energy Publications, LLC. Published by Elsevier Ltd. All rights reserved.

## Introduction

Hydrogen as energy carrier has some technical limitations that need to be addressed to promote its massive use. One major issue is hydrogen storage, owing to its low density and high chemical reactivity. Storage by means of hydrides is a feasible option, especially when considering stationary

applications. Hydride systems might be less expensive than high pressure or cryogenic storage that need a large amount of energy for compressing or liquefying the hydrogen. This results in hydride systems having lower operational cost [1].

Hydride containers are complex systems. Sorption reactions involve considerable reaction heat while the effective thermal conductivity of hydride powder is quite low. This causes important temperature changes that limit the sorption

\* Corresponding author. Centro Atómico Bariloche, Av. Ezequiel Bustillo 9500, 8400 Bariloche, Argentina. Tel.: +54 294 4445241; fax: +54 2944 4445299.

E-mail address: [silin@cab.cnea.gov.ar](mailto:silin@cab.cnea.gov.ar) (N. Silin).

<http://dx.doi.org/10.1016/j.ijhydene.2014.10.027>

0360-3199/ Copyright © 2014, Hydrogen Energy Publications, LLC. Published by Elsevier Ltd. All rights reserved.

Nomenclature			
1D	one dimensional	$\tau$	characteristic decay time, s
$\hat{C}$	pressure drop parameter, bar	T	temperature, K
$C_{sg}$	hydride capacity, kg H <sub>2</sub> /kg hydride, –	V	volume, m <sup>3</sup>
$\Delta H$	molar enthalpy of reaction, J mol <sup>-1</sup>	Subindex	
E	activation energy, J mol <sup>-1</sup>	0	fitting parameter
$\varepsilon$	hydride porosity, –	1	fitting parameter
F	heat conductive material fraction, –	90%	at 90% of total capacity
k	thermal conductivity, W m <sup>-1</sup> K <sup>-1</sup>	abs	absorption
$\hat{k}$	kinetics constant, s <sup>-1</sup>	cont	container
K	pressure drop coefficient	d	heat conductive material
L	characteristic length, m	des	desired (reaction time)
m	mass, kg	e	equilibrium
$\dot{m}$	mass flow rate, kg s <sup>-1</sup>	eff	effective
n	pressure drop exponent, –	ext	external
M	molecular weight, kg mol <sup>-1</sup>	g	hydrogen gas
NDC	non dimensional conductance, –	kin	kinetics
NDFT	non dimensional fill time, –	line	hydrogen line
NDK	non dimensional kinetics, –	max	maximum
P	pressure, bar	MH	metal hydride and interstitial hydrogen mixture
R	ideal gas constant, 8.315 J mol <sup>-1</sup> K <sup>-1</sup>	pore	pore
SS	stainless steel	s	hydride or solid
$\delta$	density, kg m <sup>-3</sup>	supply	hydrogen supply to hydride container
t	time, s	tank	hydrogen tank

reaction. When analyzing hydride containers both thermal and chemical issues has to be assessed simultaneously obtaining temperature and hydrogen concentration profiles, usually by numerical tools ([2–5] also see Table 1 in the work of Melnichuk et al. [6]). These profiles depend on the absorbing material, the container geometry and conductivity, pressure and temperature conditions and hydrogen flow through the metal hydride bulk [7]. Also in some cases, the reaction kinetics of the absorbing material cannot be disregarded.

In addition to these phenomena, which were modeled and predicted by many authors, we observe an appreciable degree of uncertainty in some parameters such as porosity and thermal conductivity of the metal hydride. Both parameters also vary during sorption reaction, for reasons such as the volume change of the particles during hydration [8]. According to sensitivity analysis, thermal conductivity of the hydride could have a significant effect on the global reaction time [9].

Therefore, considering the complexity of the physical system and the uncertainties introduced by some parameters, a simplified model providing an estimated reaction time, could be useful and even desirable in comparison to more complex models.

In this work we analyze the reaction time of a prototype hydride container using non dimensional parameters [6]. The objective of this work is to compare the estimated absorption time obtained by non dimensional analysis with experimental results, and to certain extent to validate these theoretical predictions. The container was designed based on the results of a numerical optimization that maximized the amount of hydrogen absorbed for a 3 min charging period [10]. Therefore it is expected that most of the absorption would occur during that time.

## Non dimensional parameter analysis

### Outline

In a previous work we developed a series of non dimensional parameters that provide an approximate measure of the relative importance of the different factors on the absorption process of a hydride container [6]. It is worth noting the same concepts can easily be applied to desorption dynamics. This work was based on the non dimensional conductance (NDC) defined by Visaria et al. [9], which can be regarded as the approximate ratio between the thermal evolution time and the desired charging time.

**Table 1 – Parameters for non dimensional calculations.**

Parameter	Value	Reference
$T_{max}$ (°C)	60.9 ( $P_g = 30$ bar)	This work
$\Delta H_{Abs}$ (J mol <sub>g</sub> <sup>-1</sup> )	27,020	This work
$C_{sg}$ (kg <sub>g</sub> /kg <sub>MH</sub> )	$1.15 \times 10^{-2}$	This work
$k_d$ (W m <sup>-1</sup> K <sup>-1</sup> )	138	[12]
$\rho_s$ (kg m <sup>-3</sup> )	$8.3 \times 10^3$	[13]
$\varepsilon$	0.5	[13]
$\kappa_{abs}$ (s <sup>-1</sup> )	59.2	[14]
$E_{abs}$ (J mol <sub>g</sub> <sup>-1</sup> )	21,170	[14]
$P_e$ (bar)	3.4 ( $T_{ext} = 0$ °C)	This work
	7.7 ( $T_{ext} = 20$ °C)	This work

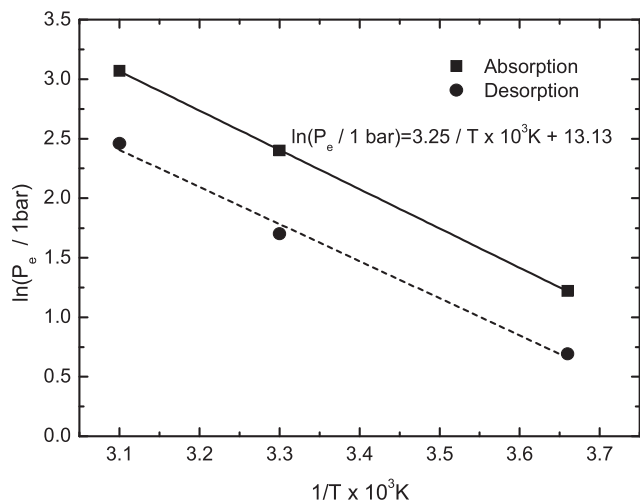


Fig. 1 – Van't Hoff chart with absorption linear fitting.

$$\text{NDC} = \frac{(T_{\max} - T_{\text{ext}})k_{\text{eff}}t_{\text{des}}}{\Delta H_{\text{abs}}C_{\text{sg}}\rho_{\text{s}}(1 - \varepsilon)(1 - F)L^2} \quad (1)$$

where:

$$k_{\text{eff}} = (1 - F)k_{\text{MH,eff}} + Fk_{\text{d}} \quad (2)$$

In other words, the NDC gives a general idea of the capability of a container to evacuate the reaction heat for a given (desired) filling time, being about unity for capable systems. We proposed a whole family of these non dimensional relations, being the most valuable from the engineering point of view the NDC and the non dimensional kinetics (NDK). The NDK accounts for the influence of the reaction kinetics as a limiting factor compared to the thermal dynamics, i.e. a large value of NDK means rapid reaction kinetics and therefore a thermally limited process while a low NDK means a reaction kinetics limitation.

$$\text{NDK} = \frac{\Delta H_{\text{abs}}C_{\text{sg}}\rho_{\text{s}}(1 - \varepsilon)(1 - F)L^2}{t_{\text{kin}}(T_{\max} - T_{\text{ext}})k_{\text{eff}}}, \quad (3)$$

where the characteristic kinetics time is defined as

$$t_{\text{kin}} = \left[ \hat{k}_{\text{abs}} e^{\frac{E_{\text{abs}}}{RT_{\text{ext}}}} \ln\left(\frac{P_{\text{g}}}{P_{\text{e}}}\right) \right]^{-1}, \quad (4)$$

Finally we defined a non dimensional fill time (NDFT) which relates the actual time it takes the container to reach 90% of its full charge to the desired fill time.

$$\text{NDFT} = \frac{t_{90\%}}{t_{\text{des}}} \quad (5)$$

In the case where dynamics is dominated only by thermal limitations, i.e. kinetics are relatively fast and therefore NDK is large, the value of NDFT can be estimated as [6]:

$$\text{NDFT} \sim 0.4/\text{NDC} \quad (6)$$

For other cases where the kinetics also acts as a limiting factor, the value of NDFT becomes larger and more difficult to estimate (see Section 3.2 of [6] for further information). We

can consider the effect of kinetics being important when NDK is lower than approximately 5. Having an estimation of NDFT, the time for the container to reach 90% of its full charge ( $t_{90\%}$ ) can be readily estimated.

### Parameter estimation

We used  $\text{MmNi}_{4.7}\text{Al}_{0.3}$  as absorbing material, given that it has higher equilibrium pressure at room temperature than  $\text{LaNi}_5$ , which was used in the previous optimization work [10]. The elements of the rare earth mixture (Mm stands for mischmetal) have variable composition and therefore the equilibrium pressure has to be determined for our particular alloy. We performed pressure-composition-temperature (PCT) measurements in a Sieverts type device to obtain parameters of the alloy used in the prototype container. With the PCT measurements we defined a Van't Hoff equation (Fig. 1), obtaining  $T_{\max}$ ,  $P_{\text{e}}$ ,  $\Delta H_{\text{abs}}$ , and  $C_{\text{sg}}$ . Density, porosity and kinetics model parameters of the hydride were assumed to be the same as  $\text{LaNi}_5$  parameters, since according to a previous sensitivity analysis [11],  $P_{\text{e}}$  and  $\Delta H_{\text{abs}}$  are among the most relevant variables for numerical calculations. These parameters are summarized in Table 1.

We analyze internal fins of our prototype made of aluminum 5052. The fins were designed to occupy close to 10% of the container internal volume, as this is the optimal relation according to the previous optimization work [10]. We also intended to make these fins as numerous and thin as possible in order to reduce the distance from the metal hydride powder to the fins surface. Yet there are technological limitations that make impractical to produce very thin fins. For this reason the fins were designed with a minimum thickness of 1.5 mm and the spacing between fins was kept to a maximum of approximately 5.5 mm. Fig. 2 on its upper left shows a scheme of the resulting design, which includes external fins to improve heat transfer to refrigerating medium. Internal design has a ratio of volume occupied by aluminum fins to the total container inner volume of 15%. In other words, the container internal volume is occupied by a 15% of aluminum fins while the metal hydride powder and the free volume occupy the remaining 85%.

The parameters for non dimensional calculation are based on a simplification of the real problem, as shown in Fig. 2. Here we will perform the analysis at two scales. The first one is the overall or macroscopic container scale, where the container is

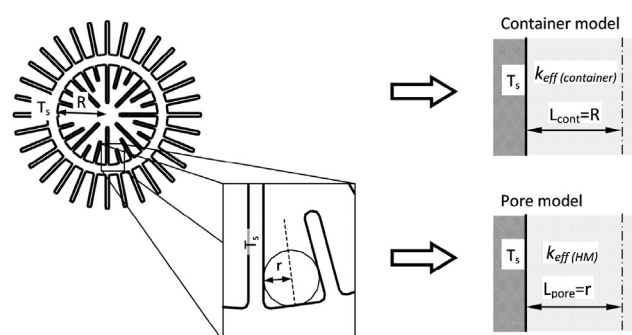


Fig. 2 – Scheme of container and pore thermal systems.

**Table 2 – Non dimensional parameters and predicted fill time calculations.**

$k_{MH_{eff}}$ ( $W m^{-1} K^{-1}$ )	Parameter	Case “A”		Case “B”	
		Container scale	Pore scale	Container scale	Pore scale
0.3	$P_g$ (bar)	30	30	30	30
	$T_{ext}$ (°C)	20	20	0	0
	$t_{des}$ (min)	3	3	3	3
	$L$ (m)	$3 \times 10^{-2}$	$2.86 \times 10^{-3}$	$3 \times 10^{-2}$	$2.86 \times 10^{-3}$
	$k_{eff}$ ( $W m^{-1} K^{-1}$ )	20.1	0.3	20.1	0.3
	(1-F)	0.85	1	0.85	1
	NDC	0.32	0.42	0.47	0.63
	NDFT	1.36	1.02	0.92	0.68
	$t_{90\%}$ (min)	<b>4.09</b>	<b>3.10</b>	<b>2.75</b>	<b>2.10</b>
	NDK	7.8	5.8	4.4	3.3
1.0	$P_g$ (bar)	30	30	30	30
	$T_{ext}$ (°C)	20	20	0	0
	$t_{des}$ (min)	3	3	3	3
	$L$ (m)	$3 \times 10^{-2}$	$2.86 \times 10^{-3}$	$3 \times 10^{-2}$	$2.86 \times 10^{-3}$
	$k_{eff}$ ( $W m^{-1} K^{-1}$ )	21.6	1	21.6	1
	(1-F)	0.85	1	0.85	1
	NDC	0.32	1.41	0.48	2.09
	NDFT	1.33	0.31	0.89	0.21
	$t_{90\%}$ (min)	<b>3.98</b>	<b>0.92</b>	<b>2.67</b>	<b>0.62</b>
	NDK	7.5	1.7	4.3	1.0

regarded as being a homogeneous material with higher effective conductivity and lower absorption capacity due to the presence of the fins. The second one is the pore or microscopic scale that involves the space between neighbor fins. The pore scale calculations consider the properties of the metal hydride powder. Non dimensional results for the two scales will provide two predicted reaction times. The slower will be the dominant scale. It should be noticed here that both scale analysis are regarded as 1D slab problems in this simplified approach, neglecting the cylindrical geometry of the container.

Moreover, we evaluated two operation scenarios: Case “A”,  $P_g = 30$  bar and  $T_{ext} = 20$  °C and Case “B”,  $P_g = 30$  bar and  $T_{ext} = 0$  °C. For the pore scale calculations, the value of the thermal conductivity of the metal hydride is very relevant, yet the value has large error margins and varies strongly with temperature and hydrogen concentration [8]. Here we decided to perform the calculations with conductivity values at the extremes of the expected value range:  $0.3 W m^{-1} K^{-1}$  to  $1 W m^{-1} K^{-1}$ .

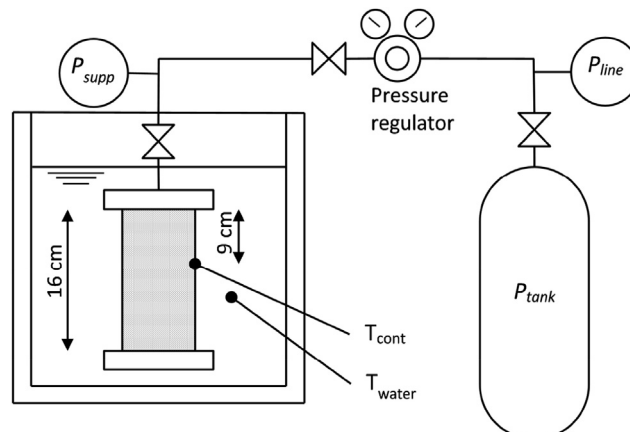
### Non dimensional parameter results

In Table 2 we show the properties, dimensions and experimental conditions needed to obtain the non dimensional parameters for the two cases and the two scales. In this table we also show the fill time ( $t_{90\%}$ ) predicted by Eq. (5) regardless NDK value. The global reaction will be dominated by the slowest process. Results show that in all cases the velocity is limited by the heat evacuation at container scale, and therefore it is not sensitive to the assumed thermal conductivity of the hydride. We can also see that for the container scale analysis the NDK values are 7.5 for Case “A” and 4.3 for Case “B”, indicating that reaction kinetics are not dominant. It is also interesting to note how sensible the pore scale calculations are to the assumed value of  $k_{MH_{eff}}$ .

### Experimental setup

The objective of the experimental setup is to provide constant pressure and unrestricted hydrogen flow to the hydride container, which is kept in a thermal bath at constant temperature. We limit our experimental analysis to container absorption time. In order to determine the time to reach 90% of full charge, mass flow rate must be measured. Due to the very wide flow range involved and the rapid variation of the flow we have decided to calculate the mass flow rate from the pressure evolution of the hydrogen supply tank.

The experimental setup is shown in Fig. 3. For the experiments we used a hydrogen tank with 99.999% purity provided by Grupo Linde Gas Argentina S.A. Tank temperature drop was measured with a PT100 probe system Testo 735. Piping installation was assembled with Swagelok ¼” SS seamless tubes and accessories. Total piping length was kept within 1 m. Pressure supply was controlled by means of a 3030-350

**Fig. 3 – Scheme of the experimental set-up.**

Matherson pressure regulator. The container was immersed in an SS water bath with recirculation and a PID temperature controller.

Temperatures were measured with type K thermocouples and pressures were measured by Omegadyne Inc. PX01 and PX01C1-1KAI pressure transducers, which were calibrated by means of a Jofa APC 05KG IND G device.

Hydride container was filled with  $(1000 \pm 3)$  g of  $MmNi_{4.7}Al_{0.3}$  melted in an arc furnace in a 99.998% argon atmosphere. To ensure homogeneity, the melting products were turned and re-melted three times. *Mm* nominal composition is: Ce 56%, La 18%, Nd 13%, Pr 5%, Fe 2%, Y 2%, other rare earths 4%. A photograph of the hydride container prototype, showing the external fins, security valve and connection system is shown in Fig. 4.

## Experimental results

Preliminary experiments showed that the measured pressure  $P_{line}$  drops immediately after the flow is established, reflecting a flow restriction at the valve and connection system of the hydrogen supply tank. This pressure drop could not be avoided in our setup for safety reasons, but we still can obtain a good estimation of the hydride container absorption time if we introduce a mathematical model for this pressure drop. In Eq. (7) we include a simplified pressure drop model to account for the difference between the measured pressure  $P_{line}$ , and the actual pressure inside the hydrogen supply tank  $P_{tank}$ .

$$P_{line} = P_{tank} - Km^n, \quad (7)$$

where  $\dot{m}$  is the mass flow rate (kg/s),  $K$  is a pressure drop coefficient, and  $n$  is an exponent to be defined. This exponent



Fig. 4 – Picture of the hydride container prototype.

depends on the type of flow and it is approximately 2 for turbulent flows and 1 for viscous creeping flows. As we do not know the fluid dynamic behavior of the valve, we will obtain this exponent from the fitting of the pressure measurements. The mass flow rate  $\dot{m}$  is related to the pressure  $P_{tank}$  by the ideal gas equation:

$$\dot{m} = \frac{dm}{dt} = \frac{MV}{RT} \left( -\frac{dP_{tank}}{dt} \right), \quad (8)$$

where  $M$  is the molar mass of hydrogen,  $R$  is the universal gas constant,  $T$  and  $V$  are the temperature and the hydrogen supply tank internal volume. Assuming that the pressure  $P_{tank}$  follows an exponential decay we obtain:

$$P_{tank} = P_0 + P_1 e^{-\frac{t}{\tau}} \quad (9)$$

where  $P_0$  is the final pressure,  $P_1$  is the total pressure change during the process and  $\tau$  is the characteristic decay time. Replacing the time derivative of Eq. (9) into Eq. (7) and then replacing this result in Eq. (7) we finally obtain:

$$P_{line} = P_0 + P_1 e^{-\frac{t}{\tau}} - \hat{C} \left( \frac{P_1}{\tau} \right)^n e^{-\frac{nt}{\tau}} \quad (10)$$

where  $\hat{C} = K(MV/RT)^n$ . This equation is represented graphically in Fig. 5 and is used to fit the experimental measurements. From Eq. (9) and Eq. (8) it can be observed that  $\dot{m}$  also decays exponentially with time, with the same time constant  $\tau$  as  $P_{tank}$ . For an exponential decay, the time to achieve 90% of the decay can be calculated as:  $t_{90\%} = (-\ln(0.1)) \times \tau = 2.3026 \tau$ .

It should be noted that to fit the experimental results,  $P_0$  and  $P_1$  are obtained from pressure measurements before the experiment is started and after the experiment is finished. The other fitting parameters are obtained by least squares method.

The pressure evolution at the hydrogen supply tank exit ( $P_{line}$ , see Fig. 5) is shown in Fig. 6 for Case “A” ( $T_{ext} = 20^\circ C$ ). Pressure fluctuations were caused by the action of the pressure regulator. This was verified by interrupting the flow to the metal hydride container at different charging stages and

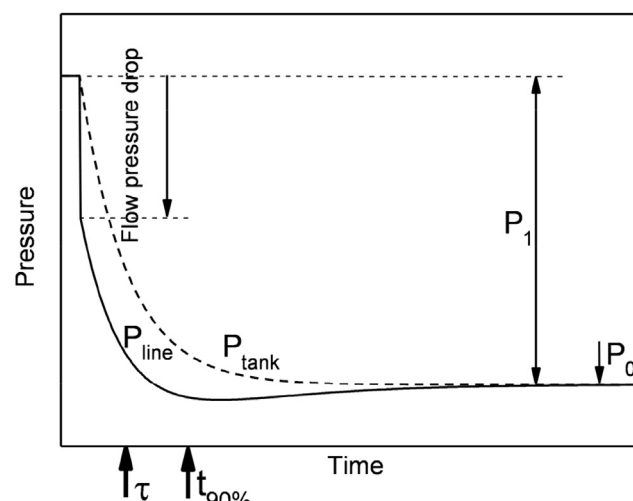
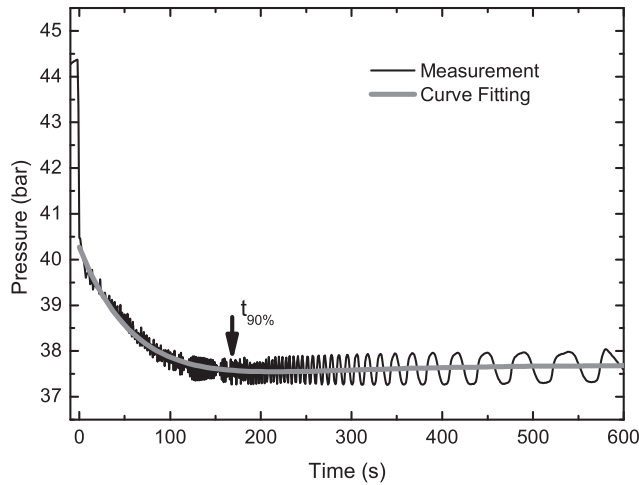
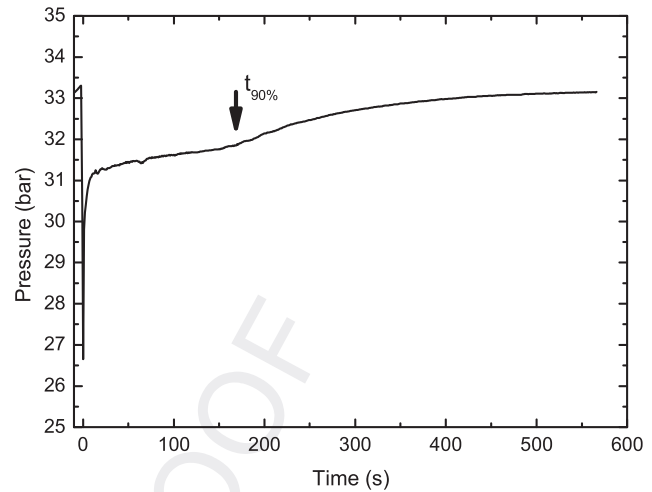


Fig. 5 – Scheme of pressure evolution model of the experimental set-up.





**Fig. 6 – Time evolution of the pressure of the hydrogen supply tank for Case “A”.**



**Fig. 7 – Time evolution of the hydrogen pressure supplied to the container for Case “A”.**

observing the immediate stabilization of the pressure  $P_{\text{line}}$ . The metal hydride container is also discarded as a source of relevant fluctuations as the hydrogen supply pressure ( $P_{\text{supply}}$ , see Fig. 3) does not show this kind of fluctuations.

The pressure behavior in Fig. 6 is characteristic, showing a sudden fall at the beginning, and then a continuous reduction of pressure that ends with some recovery. By fitting the pressure evolution with Eq. (10) we can estimate the time necessary fill the container to 90% of its capacity ( $t_{90\%}$ ). In Fig. 6 we can see the fitting curve which is in good agreement with the pressure evolution. The fitting parameters are shown in Table 3 and the resulting decay time is  $\tau = 74 \pm 7$  s. For a pure exponential decay this means  $t_{90\%} = 2.3026 \times \tau = 2.8 \pm 0.2$  min.

In Fig. 7 we show the supply pressure ( $P_{\text{supply}}$ ) evolution with time. This pressure is intended to stay constant during the experiment but shows some sensibility to the flow requirement, and the pressure recovers as the flow rate decreases with time. It is interesting to note that the pressure recovery rate increases at approximately 180 s (3 min), which is in agreement with the value of  $t_{90\%}$ .

In Fig. 8 we show the temperature evolution at the container wall and in the refrigerating water (see Fig. 3 for a reference on the locations of the temperature sensors). In this figure we can also see a change in the temperature evolution at about 180 s.

The same procedure was carried out for Case “B” ( $T_{\text{ext}} = 0$  °C). The evolution of  $P_{\text{line}}$  is shown in Fig. 9. We fitted these measurements by Eq. (10), fitting parameters are shown in Table 3. It is worth noticing that while  $P_0$ ,  $P_1$  and  $t_1$  depend on the initial pressure and the hydrogen container dynamics,  $C$

and  $n$  correspond to the flow obstruction at the outlet of the hydrogen supply tank. The two values are similar for the two cases but not equal within error margins, this is probably due to the difference in the supply tank pressure (see  $P_{\text{tank}}$  in Table 4) which causes different gas densities between the two cases. We can also see that the pressure drop for the two cases have good agreement, as the same mass of hydrogen is supplied to the container in both cases. Case “A” was performed before Case “B”, therefore  $P_{\text{tank}}$  is lower. For Case “B” the resulting decay time is  $\tau = 57 \pm 3$  s, which corresponds to  $t_{90\%} = 2.2 \pm 0.2$  min.

We have calculated the total hydrogen consumption (i.e. the capacity of the metal hydride container) knowing the pressure and temperature at the beginning and at the end of the experiment, and the supply tank internal volume ( $4.09 \pm 0.1 \times 10^{-4}$  m<sup>3</sup>). Results are shown in Table 4, where the absorbed hydrogen masses ( $\Delta m_g$ ) are equal for the two cases.

## Discussion

We analyzed two different scales: the container scale, where hydride and aluminum fins are considered as a homogeneous medium, and the pore scale, where the hydride between fins is analyzed. These two analyses bring different non dimensional parameters that show which scale and what mechanism is limiting the absorption dynamics.

The thermal conductivity of metal hydrides has a high level of uncertainty. In this work we perform two analyses, one with the highest expected conductivity and one with the lowest, obtaining a range of possible outcomes. In this

**Table 3 – Curve fitting parameters for Eq. (10).**

	$P_0$ (bar)		$P_1$ (bar)		$\tau$ (s)		$\hat{C}$ (s <sup>2</sup> /bar)		$n$	
	Value	Error	Value	Error	Value	Error	Value	Error	Value	Error
Case “A”	37.7	0.3	6.7	0.3	74	4	23	2	0.72	0.02
Case “B”	49.2	0.3	6.8	0.3	57	3	17	1	0.63	0.02

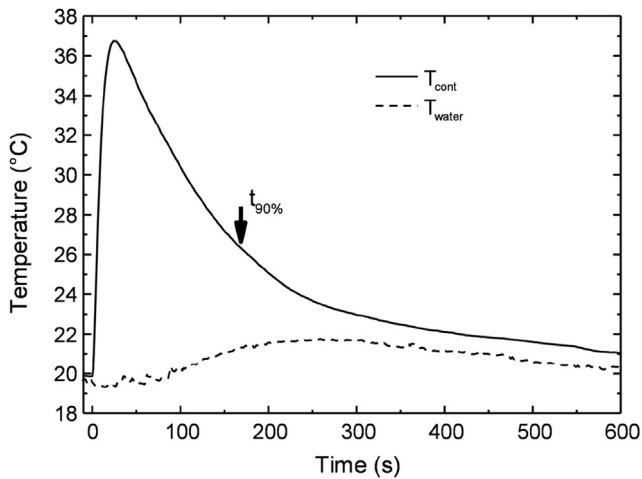


Fig. 8 – Temperature at the container wall and in the refrigerating water for Case “A”.

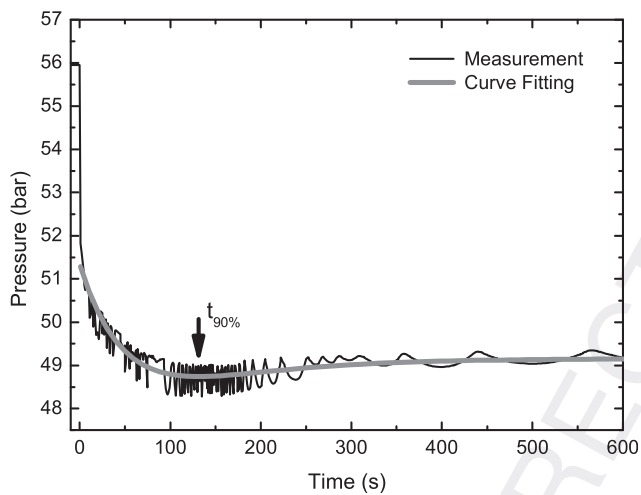


Fig. 9 – Time evolution of the pressure of the hydrogen supply tank for Case “B”.

particular case we found that the limiting scale is the macroscopic or container scale, and therefore the results are not sensible to the metal hydride thermal conductivity.

Non dimensional parameter results of Table 2 show that in all cases the container absorption velocity is limited by the heat evacuation at container scale. We also see that the results at container scale assuming  $k_{MH_{eff}} = 0.3 \text{ W m}^{-1} \text{ K}^{-1}$  or  $k_{MH_{eff}} = 1.0 \text{ W m}^{-1} \text{ K}^{-1}$  do not differ significantly. Therefore for the present cases the uncertainty in the thermal conductivity of

Table 5 – Summary of non dimensional predictions and experimental results.

	Non dimensional prediction	Experimental results	Comparison
	$t_{90\%}$ (min)	$t_{90\%}$ (min)	Difference
Case “A”	$\approx 2.7$	$2.2 \pm 0.2$	15%
Case “B”	$\approx 4.0$	$2.8 \pm 0.2$	25%

the hydride powder is not relevant. If we compare the results of Case “A” and Case “B”, we can also see that a lower external temperature improves the heat evacuation, giving higher NDC values, but there is a compromise with slower reaction kinetics, reflected in a lower NDK. If even lower temperatures were to be used, it could happen that NDK became too low, and the reaction kinetics would also take effect slowing down the adsorption process.

In Figs. 7 and 8 we can see that the actual line pressure and external temperature for Case “A” have some discrepancies with target values ( $P_g = 30 \text{ bar}$  and  $T_{ext} = 20 \text{ }^\circ\text{C}$ ). However, if we recalculate the estimated reaction time with the actual values, we only obtain a variation of 2%.

Table 5 summarizes the parametric analysis and experimental results. We can see an overestimation in the reaction time up to 25%. We consider that this tendency can be attributed to the model simplification that considers the radius of the container as the characteristic length, while the fill time calculation (Eq. (6)) assumes this length as the thickness of a 1D slab [6]. According to Eq. (1), NDC has a quadratic relation with characteristic length  $L$ . Therefore an overestimation of  $L$  results in a significant overestimation of the reaction time.

In the cases studied the overall thermal conductivity of the hydride container is satisfactory, being the measured filling time less than 3 min. This is also reflected in non dimensional parameter analysis, NFDI values being approximately 1. In other words  $t_{90\%}$  is approximately equal to the desired reaction time  $t_{des}$ .

## Conclusions

In this work we used non dimensional parameters to establish the relative importance of different phenomena on the hydrogen absorption dynamics of a prototype hydride container. This hydride container has a finned design, thus the analysis is performed at two different scales: container and pore scale, being the former the limiting scale.

We have tested the actual hydride container performance during hydrogen absorption. We found a faster absorption for lower refrigeration temperature, indicating the process is limited by the heat evacuation. For refrigeration temperature

Table 4 – Experimental results summary and  $t_{90\%}$  calculations.

	Hydrogen supply tank				Container	
	$P_{\text{tank}}$ (bar)		$T_{\text{tank}}$ ( $^\circ\text{C}$ )		$\Delta m_g$ ( $10^{-3}$ kg)	$t_{90\%}$ (min)
	Initial	Final	Initial	Final		
Case “A”	$44.4 \pm 0.3$	$37.7 \pm 0.3$	$22.6 \pm 0.3$	$21.9 \pm 0.3$	$22.1 \pm 1.8$	$2.8 \pm 0.2$
Case “B”	$56.0 \pm 0.3$	$49.2 \pm 0.3$	$9.4 \pm 0.3$	$9.1 \pm 0.3$	$23.6 \pm 2.6$	$2.2 \pm 0.2$

$T_{\text{ext}} = 20^\circ\text{C}$ , 90% fill time is  $(2.8 \pm 0.2)$  min, while for  $T_{\text{ext}} = 0^\circ\text{C}$  it is  $t_{90\%} = (2.2 \pm 0.2)$  min. This is a very satisfactory result as the container design was thermally optimized with a similar metal hydride for a 3 min absorption period [10].

Finally we have estimated the time for the container to reach 90% capacity according to non dimensional parameters. These predictions are in good agreement with the experimental results, but show some overestimation of the absorption time. This can be attributed to the cylindrical geometry which is more benign than the slab geometry assumed in the simplified model.

We think that present results show that the non dimensional parameter analysis is a useful tool for hydride container design and analysis at a preliminary stage. Better results would need not only a more sophisticated model but also a good knowledge of the properties of the metal hydride, not always available to the designer.

## Acknowledgments

The authors wish to thank the collaboration of the following people: Eng. María Eugenia Castro from Invap S.E. for prototype surface treatment, Dr. Gabriel Meyer from CNEA for the pressure calibration, Dr. Silvina Ramos from INIFTA for helping with the experimental setup and container activation, Mr. Javier Villacura and Mr. David Salas from CNEA for the assembly of the container and technical assistance. This work was done with the financial support of the Argentinean institutions Conicet, CNEA and Mincyt (PAE-PICT 2007-2164).

## REFERENCES

- [1] Jepsen J, Bellosta von Colbe JM, Klassen T, Dornheim M. Economic potential of complex hydrides compared to conventional hydrogen storage systems. *Int J Hydrogen Energy* 2012;37:4204–14.
- [2] Meng X, Bao Z, Wu Z, Yang F, Zhang Z. A comprehensive performance evaluation index for metal hydrides reactor. *Energy Procedia* 2012;29:421–30.
- [3] Nyamsi SN, Yang F, Zhang Z. An optimization study on the finned tube heat exchanger used in hydride hydrogen storage system – analytical method and numerical simulation. *Int J Hydrogen Energy* 2012;37:16078–92.
- [4] Wu Z, Yang F, Zhang Z, Bao Z. Magnesium based metal hydride reactor incorporating helical coil heat exchanger: simulation study and optimal design. *Appl Energy* 2014 [in press].
- [5] Bao Z, Yang F, Wu Z, Nyallang Nyamsi S, Zhang Z. Optimal design of metal hydride reactors based on CFD–Taguchi combined method. *Energy Convers Manag* 2013;65:322–30.
- [6] Melnichuk M, Silin N. Guidelines for thermal management design of hydride containers. *Int J Hydrogen Energy* 2012;37:18080–94.
- [7] Chung CA, Ho C-J. Thermal–fluid behavior of the hydriding and dehydriding processes in a metal hydride hydrogen storage canister. *Int J Hydrogen Energy* 2009;34:4351–64.
- [8] Hahne E, Kallweit J. Thermal conductivity of metal hydride materials for storage of hydrogen: experimental investigation. *Int J Hydrogen Energy* 1998;23:107–14.
- [9] Visaria M, Mudawar I, Pourpoint T, Kumar S. Study of heat transfer and kinetics parameters influencing the design of heat exchangers for hydrogen storage in high-pressure metal hydrides. *Int J Heat Mass Transf* 2010;53:2229–39.
- [10] Melnichuk M, Silin N, Peretti HA. Optimized heat transfer fin design for a metal-hydride hydrogen storage container. *Int J Hydrogen Energy* 2009;34:3417–24.
- [11] Melnichuk M, Andreasen G, Corso HL, Visintin A, Peretti HA. Study and characterization of a metal hydride container. *Int J Hydrogen Energy* 2008;33(13):3571–5.
- [12] Alcoa\_Insert\_5052and6061\_FINAL.pdf [http://www.alcoa.com/mill\\_products/catalog/pdf/Alcoa\\_Insert\\_5052and6061\\_FINAL.pdf](http://www.alcoa.com/mill_products/catalog/pdf/Alcoa_Insert_5052and6061_FINAL.pdf). Access: 2014-03-31 10:29:08.
- [13] Laurencelle F, Goyette J. Simulation of heat transfer in a metal hydride reactor with aluminium foam. *Int J Hydrogen Energy* 2007;32:2957–64.
- [14] Sandrock G. A panoramic overview of hydrogen storage alloys from a gas reaction point of view. *J Alloys Compd* 1999;293–295:877–88.